Aerodynamic performances of cruise missile flying above local terrain

A Ahmad, M R Saad*, A Che Idris, M R A Rahman and S Sujipto

Department of Mechanical Engineering, Faculty of Engineering, Universiti Pertahanan Nasional Malaysia, Malaysia

*rashdan@upnm.edu.my

Abstract. Cruise missile can be classified as a smart bomb and also Unmanned Aerial Vehicle (UAV) due to its ability to move and manoeuvre by itself without a pilot. Cruise missile flies in constant velocity in cruising stage. Malaysia is one of the consumers of cruise missiles that are imported from other nations, which can have distinct geographic factors including their local terrains compared to Malaysia. Some of the aerodynamic performances of missile such as drag and lift coefficients can be affected by the local geographic conditions in Malaysia, which is different from the origin nation. Therefore, a detailed study must be done to get aerodynamic performance of cruise missiles that operate in Malaysia. The effect of aerodynamic angles such as angle of attack and side slip can be used to investigate the aerodynamic performances of cruise missile. Hence, subsonic wind tunnel testings were conducted to obtain the aerodynamic performances of the missile at various angle of attack and sideslip angles. Smoke visualization was also performed to visualize the behaviour of flow separation. The optimum angle of attack found was at α=21° and side slip, β=10° for optimum pitching and yawing motion of cruise missile.

1. Introduction

Missile invention started during World War II when the first V-1 flying bomb was launched and hit London in 13th June 1944 by German forces. Then, the German army engineering team developed a new era of ballistic missiles through the successor of V-1 called V-2 (Vengeance Weapon 2) that can reach supersonic speed with over Mach 3, which means it can travel 270 km in only five minutes [1]. During the cold war between USA and Russia, weapon technology has developed rapidly between the two superpower nations that represent the capitalists and the communists block, producing a lot of modernized weapon during that time [2]. The race of technology was also seen happening until now, including in the field of aeronautics and missile systems [1, 2, 3].

Cruise missile motion is different from artillery shell like mortar. This is because the artillery shell behaves as a projectile, where its initial velocity and projection angle must be predetermined in order to deliver the shell to the target based on the range required. On the other hand, cruise missiles manoeuvre in trajectory motion that has its own flight path based on the range and speed capability. Cruise missiles operate in four stages: climb, cruise, dive and run-in [4]. Climbing is the phase when the missile flies in vertical axis to achieve the required altitude before cruising. Cruising is when the missile travels in constant velocity and close to zero acceleration. Diving stage is when the missile manoeuvres in yaw motion towards lower altitude to avoid detection by radar and being intercepted by

the air defence system. This movement requires high-g manoeuvres and decreases the total mission range capability due to high consumption of fuel. The final stage is run-in phase before hitting the target. Missiles are also capable to travel on very low altitude to avoid interception with the air defence system.

Every flying object that has symmetrical shape and fuselage needs angle of attack to generate lift [5]. Similarly, missile requires an angle of attack to launch it to the air. Basically, most of the cruise missile have symmetrical shape. Thus the presence of the angle of attacks, α is vital in producing lift for the initial movement at the launch platform to ensure that the missile will travel at the required altitude [6]. The incoming air velocity will push the surface area of an object that has an angle of attack and produce lift that is beneficial for the object to increase its altitude. High velocity of air will generate high value of lift force. This will result in high rate of climb of the flying object [6]. The values of angle of attack also affect the lift force generated. The value of angle of attack is directly proportional to the lift coefficient until at a certain angle where aerodynamic stall causes the decrease in lift coefficient [5]. Angle of slip, β is an angle between the center of fuselage and the direction of air flow. This angle occurs when the missile performs yaw motion in manoeuvre [8]. When avoiding the obstacles in the trajectory path, missile usually uses yaw and pitch motions involving angle of slip and attack [9]. Angular motion that occurs on y-axis is called pitching motion, which involves angle of attack. On the other hand, angular motion on z-axis is called yawing motion, which involves the sideslip angle [9].

The main objective of this study is to investigate the effects of angle of attack and side slip on the aerodynamic performances of cruise missile. In addition to that, the optimum angle of attack and side slip for cruise missile are also investigated, which will then lead to the determination of the suitability of the cruise missile when flying above local terrain.

2. Methodology

2.1. CAD of Tomahawk cruise missile model

Solidworks software was used to generate CAD drawing for Tomahawk Cruise Missile. The drawing was based on the real dimensions for Tomahawk cruise missile. Scale 1:20 was used in order to suit the model for print scale in the 3D printer. The wingspan for this missile was 178 mm and the overall length was 275mm. The diameter of the fuselage of the missile was 31 mm and the fin length was 90 mm. The isometric view for this missile is shown in Figure 1.

2.2. Model fabrication

3D printing, also known as Additive Manufacturing (AM), relates to many processes used to make and fabricate a three-dimensional object. In 3D printing, successive layers of material are formed under computer control to create an object. These objects can be of almost any shape or geometry, and are produced from a 3D model but with limited size of model. Poseidon-X 3D Printer was used to print the missile model with the same scale as the drawing in Figure 1. CURA software was used to import the CAD file from Solidworks. The printing process took 6 hours to complete. PLA type filaments were used as the base material in producing this model. Figure 2 shows the completed missile model with support and bracket.

2.3. Wind tunnel testing

Longwin LW-9300R subsonic wind tunnel shown in Figure 3 was used for the experiments. The speed of air that can be generated by this wind tunnel is from 1 m/s to 105 m/s. The speed of the flow was set based on the desired Reynolds number of 173,749. Dimensions for the test section of the wind tunnel is 30 cm in wide, 30 cm in height and 100 cm in length. This wind tunnel is an open-loop suction type wind tunnel. Upstream flow is sucked from outside by the rotor of wind tunnel located downstream to generate flow towards the test section. This wind tunnel is capable to measure static pressure, total pressure and speed by Pitot static pressure probe, and differential pressure meter with accuracy of

<0.25%. Lift and drag forces are measured by a three-component force balance system located at the bottom of the test section. 2D flow visualization can be conducted by the laser and smoke generator configuration as shown in Figure 4. The mounting of the model inside the test section is as shown in Figure 5.

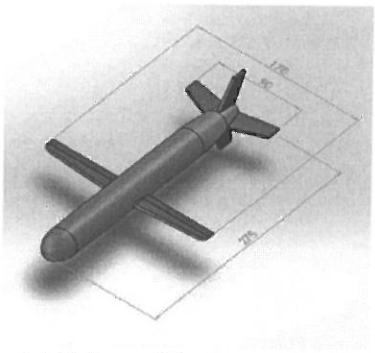

Figure 1. CAD model of Tomahawk cruise missile model

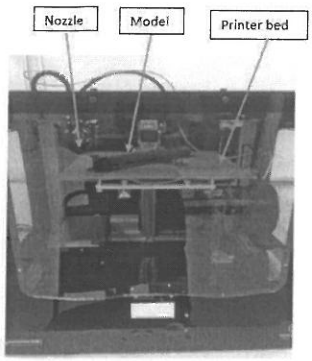

Figure 2. Fabrication of model using 3D printer

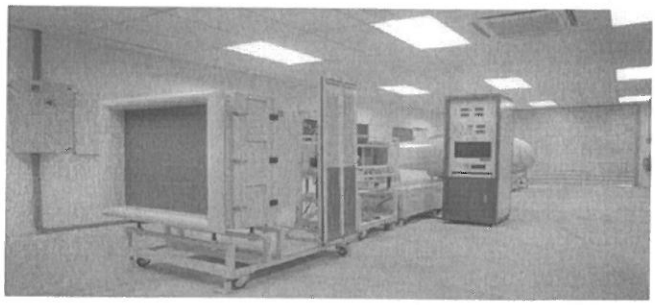

Figure 3. LW-9300R subsonic wind tunnel in UPNM

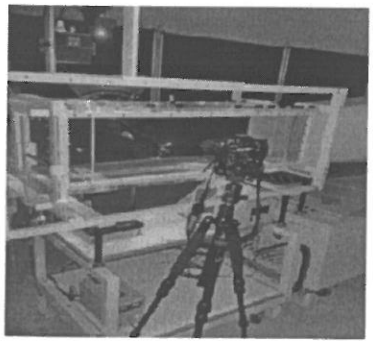

Figure 4. Recording process of flow visualization

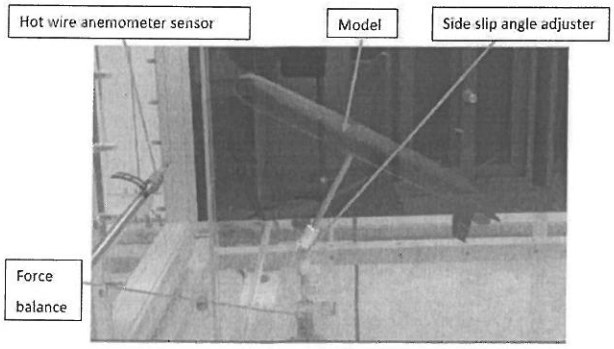

Figure 5. Installation of missile model at side slip angle, β=20° in 3 component force balance

3. Results and discussions

3.1. Validation analysis

The validation process is conducted in order to ensure that the experimental setup is able to reproduce a similar result from the established data. Figure 6 shows the graph of F_L/F_D against angle of attack, α of the experiments being compared with theoretical results obtained from Fleeman [10]. The results

from Fleeman were selected based on the similarities of the fuselage geometry used in this study. From the comparison, it can be observed that the results matched the theoretical data with slight errors as calculated in Table 1.

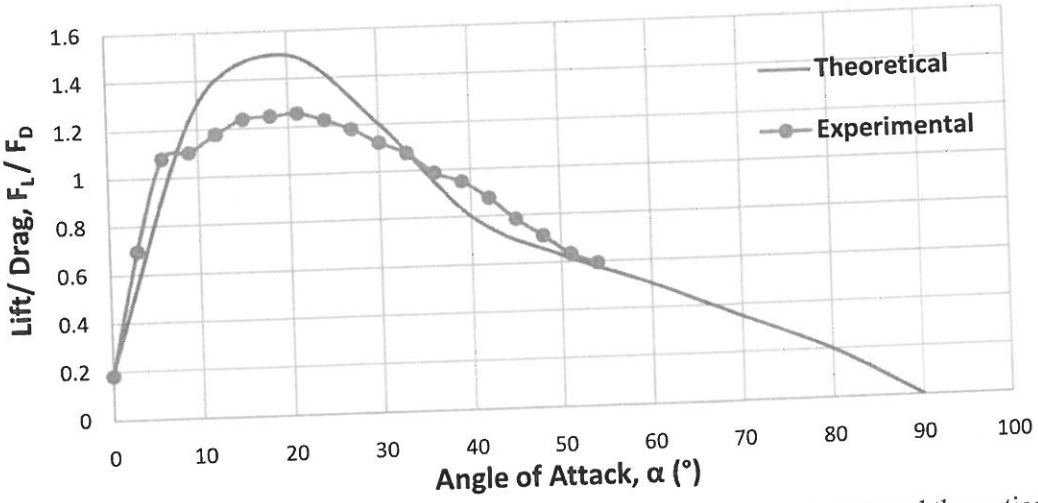

Figure 6. Comparison of F_L/F_D against angle of attack, α between experiment and theoretical

Table 1. Percentage of error between theoretical and experimental

Angle of Attack, α (°)	F_L/F_D Theoretical	F_L/F_D Experimental	Error, ϵ (%)
0	0.20	0.18	9.5
10	1.30	1.18	9.2
20	1.50	1.25	16.7
30	1.20	1.12	6.7
40	0.80	0.86	7.5
50	0.63	0.64	0.8

A few reasons that might have caused the error. Firstly, it might be due to the angle of attack of the missile model inside the wind tunnel. There was no definite method in positioning the missile model at 0° angle of attack, so an estimation was done when placing the missile model on the force balance. In addition to that, during the calibration of the force balance, there was a small error margin. This could also had an effect on the drag force results. Furthermore, the surface finishing of the missile model after fabrication was not completely smooth. Due to this, the surface had to be sand-papered. However even after using sand paper, the surface was still not completely smooth. Because of this, the results' accuracy might have reduced slightly. From another point of view, some of the minor dimensions of the model from Fleeman [10] were unknown, hence careful estimations were made for the actual wind tunnel model. This could also contribute to the errors. The highest percentage error recorded was at the angle of attack, α=20° that corresponded to 16.7% of error between the theoretical and experimental values. This might be due to the slight vibration on the model setup because of the drag induced at that specific angle of attack. On other hand, the lowest percentage of error was found at angle of attack, α=10°, accounting for 0.8% of error between the theoretical and experimental values. Overall, the errors recorded were considered to be within acceptable range.

3.2. Effect of angle of attack on lift and drag

Table 2 shows the tabulation of the results obtained for angles of attack (from 0° to 54°) of the model inside the wind tunnel for Reynolds number 173,749. C_L and C_D values were calculated from F_L and F_D that were obtained from the force balance, respectively. Please note that the uncertainty of the readings of the F_D and F_L is ± 0.01 N.

Table 2. Tabulation of aerodynamic coefficient in the variation of angle of attack

Angle of Attack, α (°)	Drag Force, F_D (N)	Lift Force, F_L (N)	Drag Coefficient, C_D	Lift Coefficient, C_L	F_L/F_D
0	0.21	0.04	0.31	0.06	0.19
3	0.23	0.16	0.32	0.23	0.70
6	0.25	0.26	0.35	0.38	1.08
9	0.28	0.31	0.41	0.45	1.10
12	0.33	0.39	0.48	0.56	1.18
15	0.37	0.46	0.54	0.66	1.24
18	0.44	0.54	0.63	0.78	1.25
21	0.50	0.63	0.72	0.0	1.26
24	0.56	0.70	0.82	1.00	1.22
27	0.65	0.76	0.93	1.10	1.18
30	0.73	0.81	1.04	1.17	1.12
33	0.78	0.84	1.13	1.21	1.08
36	0.87	0.86	1.25	1.24	0.99
39	0.95	0.90	1.37	1.30	0.95
42	1.03	0.90	1.48	1.29	0.88
45	1.14	0.89	1.64	1.28	0.78
48	1.23	0.87	1.76	1.25	0.71
51	1.31	0.83	1.89	1.20	0.63
54	1.32	0.78	1.90	1.13	0.59

Based on Figure 7, the trend of lift-to-drag ratio that increased proportionally to the angle of attack from 0° to 9° can be observed. The values then slightly increased between the angles of attack from 9° to 21°. After that, it started to decrease constantly from angle of attack of 21°. From the figure, the optimum angle of attack can be determined based on the highest value of lift to drag ratio, which is at 21°. This angle corresponds to the highest value of F_L/F_D and it can be taken as the best angle for pitching movement of missile when flying. The range of angles of attack from 15° to 24° is found to be the most effective for pitching movement of cruise missile. From Figure 8, value of lift coefficient increased in direct proportional manner with angles of attack from 0° to 39°. It started to decrease constantly after angle of attack of 39° and this phase is known as the stalling phase. Stalling phase is the loss of lift due to the factors of beyond the limitation of angle of attack in pitching.

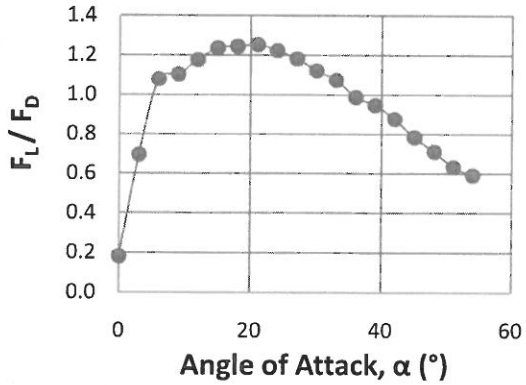

Figure 7. Graph of lift to drag ratio against angle of attack

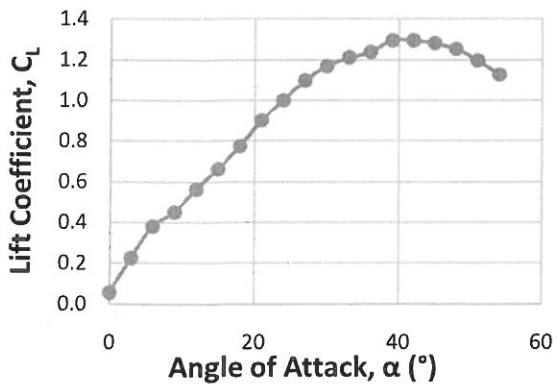

Figure 8. Graph of relationship between lift coefficient and angle of attack

3.3. Effect of side slip angle on lift and drag

Lift and drag coefficients are heavily influenced not only by the angle of attack but also the side slip angle. This is proven from the data collected and tabulated in Table 3, which shows the tabulation of aerodynamic coefficients on the variation of side slip angle experiment where the angle of attack was

set constant at 0°. The side slip angle of the model was adjusted inside the wind tunnel using the side slip adjustor, connecting the model to the mounting rod as previously shown in the setup in Figure 8.

Table 3. Tabulation of aerodynamic coefficient in the variation of side slip angle

Angle of Side Slip, β (°)	Drag Force, F_D (N)	Lift Force, F_L (N)	Drag Coefficient, C_D	Lift Coefficient, C_L	F_L/F_D
0	0.09	0.02	0.13	0.03	0.22
5	0.10	0.02	0.14	0.03	0.20
10	0.11	0.05	0.16	0.07	0.45
15	0.13	0.01	0.18	0.01	0.08
20	0.28	0.00	0.41	0.00	0.00
25	0.30	-0.01	0.44	-0.01	-0.03
30	0.32	-0.02	0.47	-0.03	-0.06

Figure 9 shows the relationship between lift coefficient and side slip angle from angle of attack of 0° to 30°. Based on the figure, initially the lift coefficient slightly decreased from the side slip angle of 0° to 5°. Then, it increased rapidly starting from 5° to 10°. After that, the value went down as the side slip angle increased. The peak value recorded for lift coefficient was at the side slip angle, β= 10°. Beyond the value of β = 20°, the missile lost its lift and entered the stall region. The graph of drag coefficient with relation to side slip angle is shown in Figure 10. Based on the figure, drag coefficient value in overall increased with respect to the side slip angle. The drag coefficient increased marginally from side slip angle of 0° to 15°. Then, it suddenly underwent rapid increase from side slip angle of 15° to 20°. Finally, it slowly increased from side slip angle of 20° to 30°.

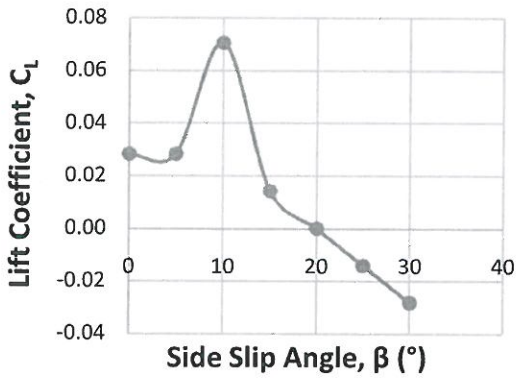

Figure 9. Graph of relationship between lift coefficient and side slip angle

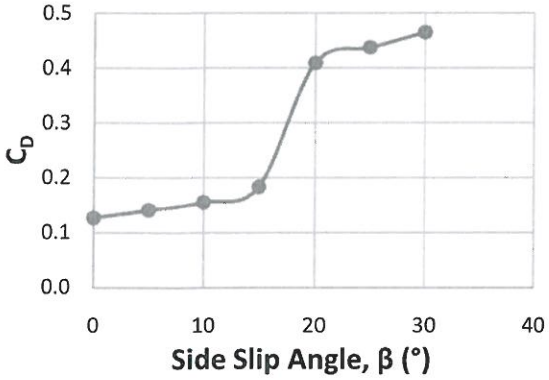

Figure 10. Graph of relationship between drag coefficient and side slip angle

Figure 11 shows the lift-to-drag ratio plot against the side slip angle. Based on the figure, there are three types of trend that can be observed from the plotted values. The first one is the slightly decrease of lift-to-drag ratio value from side slip angles of 0° to 5°. Then, the lift-to-drag ratio value increasing rapidly starting from side slip angles of 5° to 10°. After that, the value went down as the side slip angle increases. Hence, the optimum side slip angle for yawing determined from Figure 11 is at 10° due to the highest value of lift to drag ratio.

As a summary for this analysis, the optimum value for side slip angle, β was able to be determined, which was at 10°. This was useful in configuring the yawing motion of the missile. Besides that, the limitation angle for the missile to yaw before reach a stalling phase was also observed from the data, where side slip angle above 20° can be considered as not safe for missile manoeuvres.

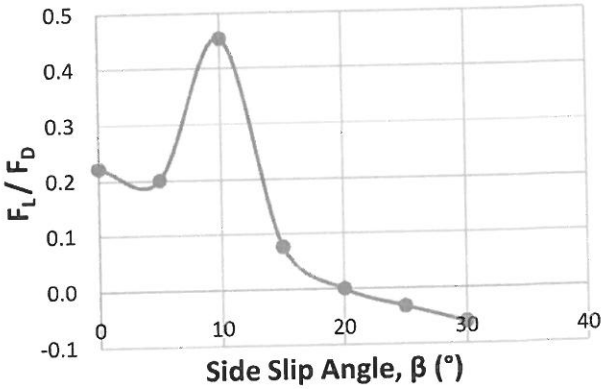

Figure 11. Graph of lift to drag ratio against side slip angle

3.4. Flow visualization results

The flow visualization experiment was conducted at velocity of 1.6 m/s to visualize the behaviour of the boundary layer on the missile body at various angles of attack ranging from 10° to 30°. Figure 12 indicates the location of the separation points on the model at different angles of attack.

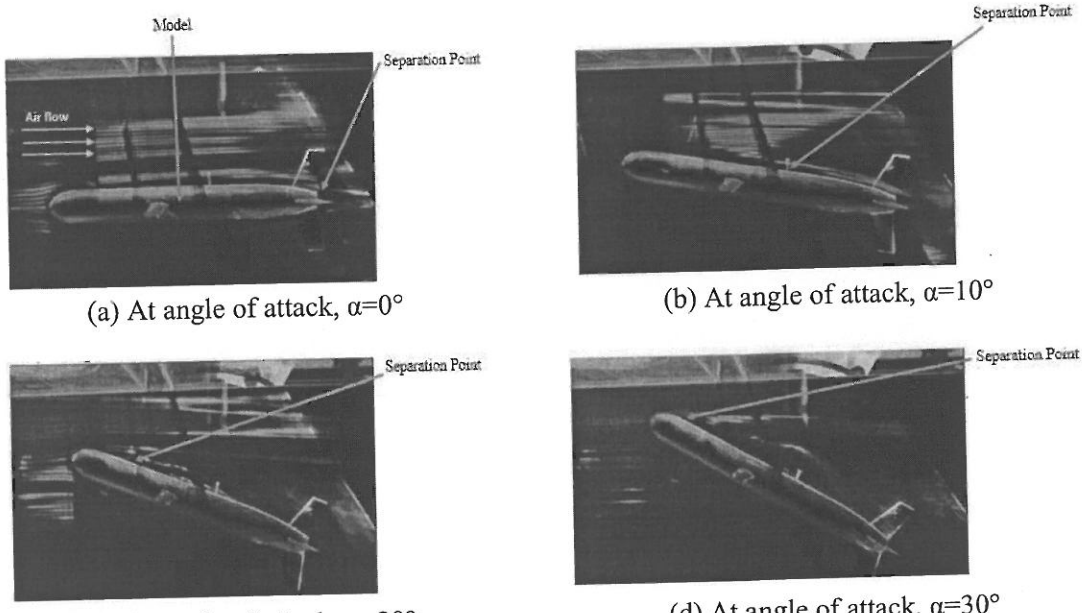

(a) At angle of attack, α=0°

(b) At angle of attack, α=10°

(c) At angle of attack, α=20°

(d) At angle of attack, α=30°

Figure 12. Photos of flow visualization experiments on missile model at various angles of attack

From the images in Figure 12, it can be seen the difference of flow trajectory between each of angle of attack increment. As an example, the separation point for 0° of angle of attack was at the rear region near the fin but by increasing angle of attack, the separation point was found to shift to the upstream of the fuselage. This in turn will cause large separation region that eventually contributed to the increase of the drag force. The separation point marks the starting point of turbulent eddies that occurred on the fuselage of missile model. This is the main reason why the increased of angle of attack also increases the value of drag coefficient as shown by the data in Figure 10.

3.5. Pitching motion analysis

Malaysian terrain has no permanent pasture or prairie land. Hills and mountains mostly dominate the Malaysian terrain that have an average elevation of 1,829 meters. This will cause a lot of manoeuvring for the missile to climb and avoid itself from hitting any obstacles such as hills or mountains. Thus, by determining the optimum angle of attack based on Table 4, the missile is able to plan its movements by avoiding obstacles and manoeuvring at the most efficient aerodynamic performances. Figure 13 presents a simple pitching analysis done on the combination of angle of attack and the climb that the missile needs to make in order to avoid an obstacle of 1,829 m high. From the figure, the distance, D can be calculated that translates into the point before the obstacle where the missile needs to pitch up.

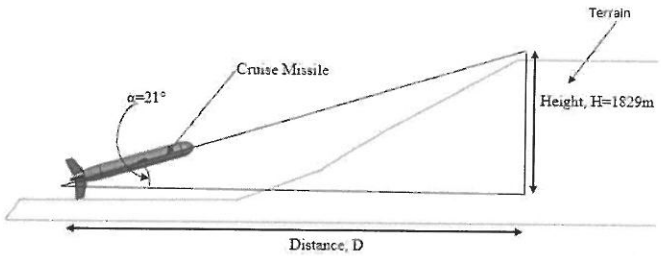

Figure 13. Pitching analysis on optimum angle of attack

Table 4. The optimum aerodynamic angles

Type of Angle	Optimum Angle (°)
Angle of Attack	21
Side Slip Angle	10

4. Conclusion

The experiments conducted in the wind tunnel provides the data for aerodynamic performances of the cruise missile model. The optimum values found for angle of attack was at $\alpha=21°$ and side slip angle at $\beta=10°$ for pitching and yawing motion of the missile from maximum ratio of lift to drag data for this two aerodynamic angles. The flow visualization shows the existence of flow separation that represents the starting point of vortices and turbulent eddies that causes induced drag due to increment of angle of attack. Finally, a simple dynamic analysis was performed by calculating the required distance as a guideline for the missile to start climbing for the optimum angle of attack to avoid from hitting high obstacles like hills and mountains when flying above Malaysian terrain.

Acknowledgements

The authors would like to thank Ministry of Education Malaysia for financial support under the RAGS (RAGS/1/2014/TK09/UPNM/1) and RACE (RACE/F3/PK6/UPNM/13) research grant schemes. Also, an appreciation to technical staffs of Faculty of Engineering, Universiti Pertahanan Nasional Malaysia for providing the assistances to the equipment.

References

[1] De Vorkin D H and Neufeld M J 2011 *Endeavour* **35** 187-95
[2] Eckersley C F 2009 *47th AIAA Aerospace Sciences Meeting*
[3] Adams D, Criss T B and Shankar U J 2008 *IEEE Aerospace Conference*
[4] Krieger R 1982 *9th Atmospheric Flight Mechanics Conference*
[5] Zastawny M, Mallouppas G, Zhao F and Wachem B 2012 *International Journal of Multiphase Flow* **39** 227-39
[6] Ma Y, Guo J and Tang S 2015 *Journal of Aerospace Science and Technology* **45** 324-34
[7] Riedel F 1941 *Guidance and Control Conference*
[8] Jouannet C and Krus P 2007 *25th AIAA Applied Aerodynamic Conference*
[9] Anderson J D 2016 *Introduction to Flight* (New York: McGraw-Hill)
[10] Fleeman E L 2006 *Tactical Missile Design* (Reston: AIAA)